Modeling Graphene in the Finite-Difference Time-Domain Method Using a Surface Boundary Condition

Vahid Nayyeri, *Student Member, IEEE*, Mohammad Soleimani, and Omar M. Ramahi, *Fellow, IEEE*

***Abstract*—An effective approach for finite-difference time-domain modeling of graphene as a conducting sheet is proposed. First, we present a new technique for implementing a conducting surface boundary condition in the FDTD method; then, the dispersive surface conductivity of graphene is imposed. Numerical examples are presented to show the stability, accuracy, applicability, and advantages of the proposed approach. Validation is achieved by comparison with existing analytic methods.**

***Index Terms*—Finite-difference time-domain (FDTD), graphene, surface boundary condition.**

I. Introduction

GRAPHENE, which is a planar monoatomic layer of carbon bonded in a hexagonal structure, has recently gained significant interest due to its potential in enabling new technologies and addressing key technological challenges [1], [2]. In response to electromagnetic fields, graphene behaves as a surface with conductivity that depends on chemical doping or external field bias [3], [4]. To understand the scattering and wave guiding properties of graphene, Maxwell equations need to be solved either in two-dimensional or three-dimensional space. Analytical solutions for simple canonical problems involving graphene layers are available; however, for most problems, numerical solutions of Maxwell equations are inevitable. Vakil and Engheta [5] proposed considering graphene sheet as a very thin layer (with thickness around 1 nm) and the surface conductivity of graphene to be converted to volumetric conductivity. Due to simplicity and applicability to most numerical methods (particularly, applicability to most popular commercial software tools such as CST Studio Suite [6] and COMSOL Multiphysics [7]), the technique proposed by Vakil and Engheta was used in most of the published works such as [8]–[13]. Since the space inside the graphene layer has to be finely meshed, the solver needs significant computing memory resources and time. Since the graphene sheet has practically zero thickness, it can be modeled as a surface boundary condition (SBC) as was done in earlier works [14], [15]. Although this approach is effective, its implementation is challenging in numerical methods based on volumetric discretization and requires special modification to the algorithm.

The finite-difference time-domain (FDTD) method is one the most popular numerical techniques for solving Maxwell equations because of its generality, simplicity and ease of implementation, particularly when a wide range of frequency is of interest [16], [17]. Modeling graphene in FDTD can be performed in different ways with dramatic variation in the efficiency and resource requirements of the simulation. Two approaches that were used for modeling of graphene sheets in the FDTD method are: 1) Standard FDTD method with fine enough discretization inside the sheet [8], [9], [18], [19] and 2) Subcell FDTD approach typically used to model electrically thin material sheets [20]. In both approaches, graphene sheets were considered as thin layers occupying some (in the first one) or a fraction (in the second one) of the FDTD cells while converting the surface conductivity of graphene to volumetric conductivity. Since graphene is physically one-atom-thick layer, the first approach calls for extremely fine spatial discretization of the computational domain. In the FDTD method introduced by Yee [16], because of the linear relationship between the discretization steps in space and time (related to stability), finer spatial grid needs finer time steps. Therefore, this approach requires large memory resources and time, and hence is impractical in most real-world problems. The second approach, which uses the subcell FDTD method, cannot model infinitely thin sheets, and requires special type of PML [21].

SBCs have been implemented in the FDTD method in many works; however, most of the earlier works considered only the reflection from a layer in what has become known as the surface impedance boundary condition approach [22], [23]. In 1992, Wu and Han [24] introduced a method for implementation of a resistive sheet boundary condition which handles both transmission and reflection through an infinitesimally thin resistive sheet, but the method suffered from instability [24], [25]. Other approaches were introduced for modeling a thin layer of good conductor with high loss using impedance network boundary condition [26]–[29]; however, for an infinitesimally thin layer these methods were fundamentally identical to the work by Wu

Manuscript received February 05, 2013; revised April 10, 2013; accepted April 22, 2013. Date of publication May 16, 2013; date of current version July 31, 2013. This work was supported by the Natural Sciences and Engineering Research Council of Canada, Iran Ministry of Science Research and Technology, and the Research Institute of ICT.

V. Nayyeri is with the Electrical and Computer Engineering Department, University of Waterloo, Waterloo, ON N2L 3G1, Canada and also with the School of Electrical Engineering, Iran University of Science and Technology, Tehran, Iran (e-mail: nayyeri@ieee.org).

M. Soleimani is with the School of Electrical Engineering, Iran University of Science and Technology, Tehran 16844, Iran (e-mail: soleimani@iust.ac.ir).

O. M. Ramahi is with the Electrical and Computer Engineering Department, University of Waterloo, Waterloo, ON N2L 3G1 Canada (e-mail: oramahi@uwaterloo.ca).

Color versions of one or more of the figures in this paper are available online at http://ieeexplore.ieee.org.

Digital Object Identifier 10.1109/TAP.2013.2260517

0018-926X/$31.00 © 2013 IEEE

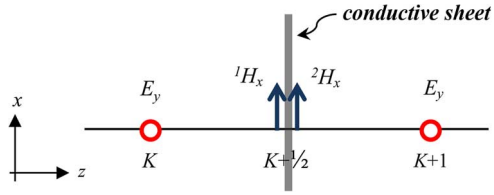

Fig. 1. A 1-D FDTD cell including a conductive sheet at grid $K+1/2$.

and Han [24]. Considering that graphene sheets are infinitesimally thin and that graphene is not a good conductor (i.e., the imaginary part of the surface conductivity of graphene is larger than its real part), the previous methods and approach are not applicable for modeling graphene as an SBC in the FDTD method.

In this paper, we propose a method for implementing an SBC in the FDTD method without any restriction on the conductivity of the surface, thus making the method directly applicable to modeling graphene. The graphene is considered as a zero-thickness sheet with complex conductivity, and the approach proposed, which is based on coupling between updating equations at both sides of the sheet, is used to implement a surface boundary condition in the FDTD method. Full validation of the method is presented.

II. Implementation of Conducting Surface Boundary Condition in the FDTD Method

A. Implementation in 1-D FDTD

We first consider the one-dimensional problem of a TEM polarized plane wave incident normally on a conducting sheet. The 1-D FDTD mesh including a conductive surface is shown in Fig. 1, where the E_y and H_x field components are staggered one-half cell apart. A conductive surface with constant conductivity σ_s is positioned at the spatial grid $K+1/2$, as shown in Fig. 1. Since a conductive material allows for the possibility of a conduction current, we consider two magnetic fields, ${}^1H_x$ and ${}^2H_x$ immediately to the left and right sides of the conductive sheet boundary. Next, we discretize Faraday's law $\partial \boldsymbol{B}/\partial \mathrm{t} = -\nabla \times \boldsymbol{E}$ at the grid $K+1/2$ such that the central difference scheme is used for the time derivative $\partial \boldsymbol{B}/\partial \mathrm{t}$, and backward and forward difference schemes are used for spatial derivative along the z direction:

$$\begin{aligned} \mu_1 \delta_t^c \left\{ {}^1H_x^n \right\} &= \delta_z^b \left\{ E_y^n(K+1/2) \right\} \\ \mu_2 \delta_t^c \left\{ {}^2H_x^n \right\} &= \delta_z^f \left\{ E_y^n(K+1/2) \right\} \end{aligned} \tag{1}$$

where μ_1 and μ_2 are the permeability of media to the left and right sides of the interface, and δ^c, δ^b, and δ^f are the central, backward and forward difference derivative approximations defined as

$$\begin{aligned} \delta_x^c\{F\} &= \frac{F(x+\Delta x/2) - F(x-\Delta x/2)}{\Delta x} \\ \delta_x^b\{F\} &= \frac{F(x) - F(x-\Delta x/2)}{\Delta x/2} \\ \delta_x^f\{F\} &= \frac{F(x+\Delta x/2) - F(x)}{\Delta x/2}. \end{aligned}$$

(1) requires the value of E_y at $(K+1/2)$, which is not defined in the FDTD mesh (see Fig. 1). However, using the boundary condition at the conducting surface,

$${}^2H_x - {}^1H_x = \sigma_s E_y$$

E_y can be substituted by

$$\begin{aligned} E_y^n(K+1/2) = \frac{1}{2\sigma_s} \Big[\left({}^2H_x^{n+1/2} + {}^2H_x^{n-1/2} \right) \\ - \left({}^1H_x^{n+1/2} + {}^1H_x^{n-1/2} \right) \Big] \end{aligned} \tag{2}$$

where the values of the magnetic field components at time step n are approximated by the average of the field values at $n-1/2$ and $n+1/2$. Rearranging (1), we have

$$\begin{bmatrix} 1 & -c_1 \\ -c_2 & 1 \end{bmatrix} \begin{bmatrix} {}^1H_x^{n+1/2} \\ {}^2H_x^{n+1/2} \end{bmatrix} = \begin{bmatrix} F_1^n \\ F_2^n \end{bmatrix} \tag{3}$$

where

$$c_1 = \frac{\Delta t}{\mu_1 \Delta z \sigma_s + \Delta t}, c_2 = \frac{\Delta t}{\mu_2 \Delta z \sigma_s + \Delta t}$$

F_1^n and F_2^n are functions of the field components at time steps n and $n-1/2$ defined by

$$\begin{aligned} F_1^n &= -2 f_{e1} E_y^n(K) + f_{h11} {}^1H_x^{n-1/2} + f_{h12} {}^2H_x^{n-1/2} \\ F_2^n &= 2 f_{e2} E_y^n(K+1) + f_{h21} {}^1H_x^{n-1/2} + f_{h22} {}^2H_x^{n-1/2} \end{aligned}$$

and

$$\begin{aligned} f_{e1} &= \sigma_s c_1, f_{e2} = \sigma_s c_2 \\ f_{h11} &= 1 - 2c_1, f_{h22} = 1 - 2c_2 \\ f_{h12} &= c_1, \text{ and } f_{h21} = c_2. \end{aligned}$$

The updating equations for ${}^1H_x$ and ${}^2H_x$ can be obtained by solving (3)

$$\begin{aligned} {}^1H_x^{n+1/2} &= \frac{1}{1-c_1c_2} \left(F_1^n + c_1 F_2^n \right) \\ {}^2H_x^{n+1/2} &= \frac{1}{1-c_1c_2} \left(F_2^n + c_2 F_1^n \right). \end{aligned} \tag{4}$$

Once the updating equations at the surface are derived, one can easily apply classical leapfrog algorithm for updating the field values at other grids, considering that ${}^1H_x$ and ${}^2H_x$ should be used for updating E_y at grids K and $K+1$, respectively.

B. Implementation in 3-D FDTD

Fig. 2 shows a 3-D FDTD cell including a conductive surface positioned parallel to the xy plane at the z grid $K+1/2$. Due to the possibility of current and net charge at the conducting surface, a pair of each of the tangential components of the magnetic field (H_x and H_y) and a pair of the normal component of electric field (E_z) are considered immediately to the bottom and top sides of the surface. The pair associated with each field are designated by the superscripts 1 and 2 (see Fig. 2). The updating equations for these components can be derived in a similar way to the 1-D case. By discretization of Faraday's law $\partial \mathbf{B}/\partial t = -\nabla \times \mathbf{E}$ at $(i, j+1/2, K+1/2)$ such that the central difference scheme is used for the time derivative and spatial derivatives along x and y direction (parallel to the surface), and

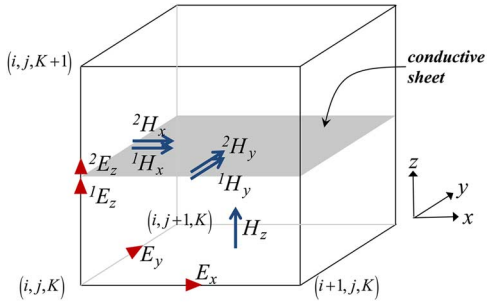

Fig. 2. A 3-D FDTD cell including a conductive sheet at grid $K+1/2$.

the backward and forward difference schemes are used for the spatial derivatives along z direction (normal to the surface), we have

$$\begin{aligned}\mu_1\delta_t^c\left\{{}^1H_x^n\right\} &= \delta_z^b\left\{E_y^n(i,j+1/2,K+1/2)\right\}\\ &\quad-\delta_y^c\left\{{}^1E_z^n(i,j+1/2,K+1/2)\right\}\\ \mu_2\delta_t^c\left\{{}^2H_x^n\right\} &= \delta_z^f\left\{E_y^n(i,j+1/2,K+1/2)\right\}\\ &\quad-\delta_y^c\left\{{}^2E_z^n(i,j+1/2,K+1/2)\right\}\end{aligned}\tag{5}$$

where μ_1 and μ_2 are the permeability of the media to the bottom and top sides of the interface. A pair of similar equations can be written for ${}^1H_y$ and ${}^2H_y$. Clearly, (5) requires E_y at $(i,j+1/2, K+1/2)$; however, this component is not defined at that grid point in the FDTD cell (see Fig. 2), therefore, it is expressed using ${}^1H_x$ and ${}^2H_x$ via the boundary condition, same as (2). Finally, a system of equations, identical to (3), can be obtained where F_1^n and F_2^n are defined as

$$\begin{aligned}F_1^n &= f_{h11}{}^1H_x^{n-1/2}+f_{h12}{}^2H_x^{n-1/2}\\ &\quad-f_{e1}\left[2E_y^n(i,j+1/2,K)+\Delta z\delta_y^c\left\{{}^1E_z^n\right\}\right]\\ F_2^n &= f_{h21}{}^1H_x^{n-1/2}+f_{h22}{}^2H_x^{n-1/2}\\ &\quad+f_{e2}\left[2E_y^n(i,j+1/2,K+1)-\Delta z\delta_y^c\left\{{}^2E_z^n\right\}\right].\end{aligned}$$

Therefore, solving (3) gives updating equations for ${}^1H_x$ and ${}^2H_x$ as (4). In a similar way, one can obtain updating equations for ${}^1H_y$ and ${}^2H_y$. Finally, ${}^1E_z$ and ${}^2E_z$ are, respectively, updated by ${}^1H_x$, ${}^1H_y$, and ${}^2H_x$,${}^2H_y$ using classical Yee's algorithm, i.e.,

$$\begin{aligned}{}^1E_z^{n+1} &= {}^1E_z^n+\frac{\Delta t}{\varepsilon_1}\left[\delta_x^c\left\{{}^1H_y^n\right\}-\delta_y^c\left\{{}^1H_x^n\right\}\right]\\ {}^2E_z^{n+1} &= {}^2E_z^n+\frac{\Delta t}{\varepsilon_2}\left[\delta_x^c\left\{{}^2H_y^n\right\}-\delta_y^c\left\{{}^2H_x^n\right\}\right].\end{aligned}$$

We tested our method for stability by using different values of σ_s. No instability was observed for $0<\sigma_s<\infty$. In the simulations we set $\Delta t=\Delta z/(\sqrt{\mathrm{N_{dim}}}\,c)$ (where $\mathrm{N_{dim}}$ is dimension of the problem and c is wave velocity in the medium) and found that the method does not affect the CFL stability condition. It should be noted that considering (4), the presented method works if $1-c_1c_2\neq 0$. Substituting the values of c_1 and c_2, we have $\sigma_s\neq 0$, which is an inherent condition.

III. Application to the Modeling of Graphene Structures

In the absence of magnetostatic bias and spatial dispersion, graphene can be represented as a scalar surface conductivity $\sigma_g(\omega,\mu_c,\Gamma,T)$ that depends on frequency ω, chemical potential μ_c (which can be controlled by either an applied electrostatic bias or doping), phenomenological scattering rate Γ, and temperature T [4]. The conductivity of graphene has been commonly expressed by the well-known Kubo formula consisting of two terms, $\sigma_g=\sigma_{\mathrm{intra}}+\sigma_{\mathrm{inter}}$, where the former is due to the intraband contributions and the latter to the interband contributions. It is shown that for the frequency below $\hbar\omega=2\mu_c$, where $\hbar$ is the reduced Planck constant, the interband term is negligible and the intraband term is dominant [3]. Considering $\mu_c>0.05$ eV, which is a practical condition, the intraband is the dominant term in gigahertz and terahertz regimes. σ_{intra} can be evaluated by Drude-like expression as in

$$\sigma_{\mathrm{intra}}(\omega,\mu_c,\Gamma,T)=\frac{\sigma_0}{1+j\omega\tau}\tag{6}$$

where

$$\sigma_0=\frac{e^2\tau k_BT}{\pi\hbar^2}\left[\frac{\mu_c}{k_BT}+2\mathrm{Ln}\left(\exp\{-\mu_c/k_BT\}+1\right)\right]$$

is the dc conductivity, $\tau=1/(2\Gamma)$ is the phenomenological electron relaxation time, e is the electron charge and k_B is the Boltzmann constant [3]. Similar to earlier works in the terahertz regime, (6) is considered as the surface conductivity model of a graphene sheet.

To implement the conductivity model [(6)] in the FDTD method, the boundary condition at a conducting sheet can be written in the frequency domain as

$$\hat{n}\times\left[{}^{\mathbf{2}}\mathbf{H}(\omega)-{}^{\mathbf{1}}\mathbf{H}(\omega)\right]=\sigma_s(\omega)\mathbf{E_t}(\omega)\tag{7}$$

where $\hat{n}$ denotes the unit vector normal to the sheet, ${}^{\mathbf{1}}\mathbf{H}$ and ${}^{\mathbf{2}}\mathbf{H}$ are magnetic fields at two sides of the sheet, $\mathbf{E_t}$ is the tangential component of the electric field at the sheet, and σ_s is the surface conductivity. By substituting (6) in (7) and converting the expression from frequency domain to time domain via $j\omega\rightarrow\partial/\partial\mathrm{t}$, we have

$$\mathbf{E_t}(t)=\frac{1}{\sigma_0}\left(1+\tau\partial/\partial t\right)\left[{}^{\mathbf{1}}\mathbf{H}(t)-{}^{\mathbf{2}}\mathbf{H}(t)\right]\times\hat{n}.$$

By using central difference scheme for time derivative, we obtain

$$\begin{aligned}\mathbf{E_t^n}=\frac{1}{\sigma_0}\hat{n}\times\Big\{&(1/2+\tau/\Delta t)[{}^{\mathbf{2}}\mathbf{H}-{}^{\mathbf{1}}\mathbf{H}]^{n+1/2}\\ &+(1/2-\tau/\Delta t)[{}^{\mathbf{2}}\mathbf{H}-{}^{\mathbf{1}}\mathbf{H}]^{n-1/2}\Big\}.\end{aligned}$$

The implementation into an FDTD algorithm will then follow the steps outlined in Section II and results in field

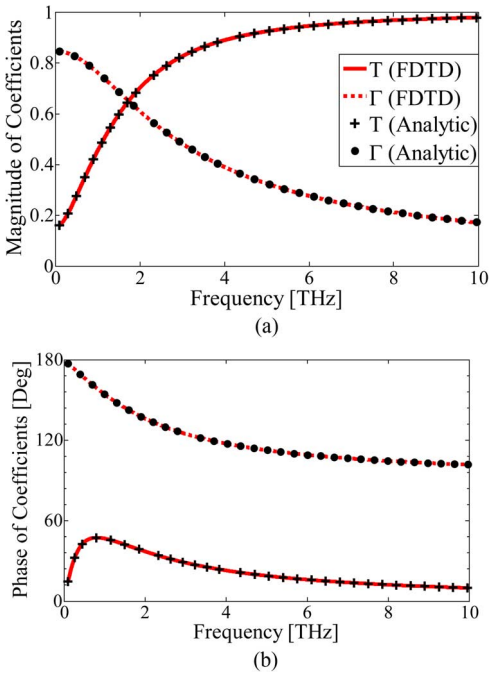

Fig. 3. Transmission (T) and reflection (Γ) coefficients for normally incident plane wave on a graphene layer, (a) magnitude, and (b) phase.

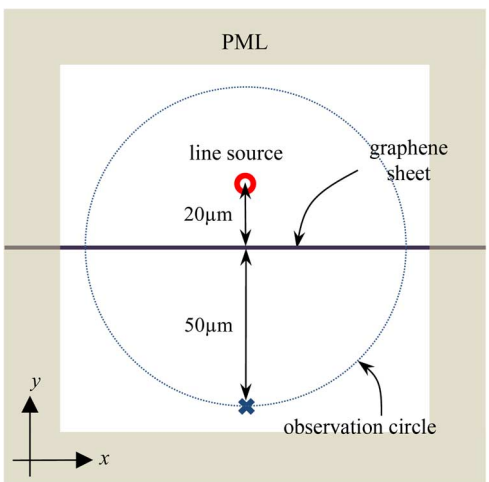

Fig. 4. Line source scattering by a graphene infinite sheet.

update equations identical to (4) aside for the following substitutions:

$$c_1 = \frac{\Delta t + 2\tau}{\mu_1 \Delta z \sigma_0 + \Delta t + 2\tau}, \qquad c_2 = \frac{\Delta t + 2\tau}{\mu_2 \Delta z \sigma_0 + \Delta t + 2\tau}$$

$$f_{e1} = \frac{\Delta t \sigma_0}{\mu_1 \Delta z \sigma_0 + \Delta t + 2\tau}, \qquad f_{e2} = \frac{\Delta t \sigma_0}{\mu_2 \Delta z \sigma_0 + \Delta t + 2\tau}$$

$$f_{h11} = 1 - \frac{2\Delta t}{\mu_1 \Delta z \sigma_0 + \Delta t + 2\tau}, \qquad f_{h22} = 1 - \frac{2\Delta t}{\mu_2 \Delta z \sigma_0 + \Delta t + 2\tau}$$

$$f_{h12} = \frac{\Delta t - 2\tau}{\mu_1 \Delta z \sigma_0 + \Delta t + 2\tau}, \qquad f_{h21} = \frac{\Delta t - 2\tau}{\mu_2 \Delta z \sigma_0 + \Delta t + 2\tau}.$$

IV. Model Validation and Simulation Results

We consider a grapheme sheet of $T = 300$ K, $\mu_c = 0.5$ eV and $\tau = 0.5$ ps, consistent with [30]. As a first example, 1-D FDTD technique is applied where a wideband Gaussian pulse

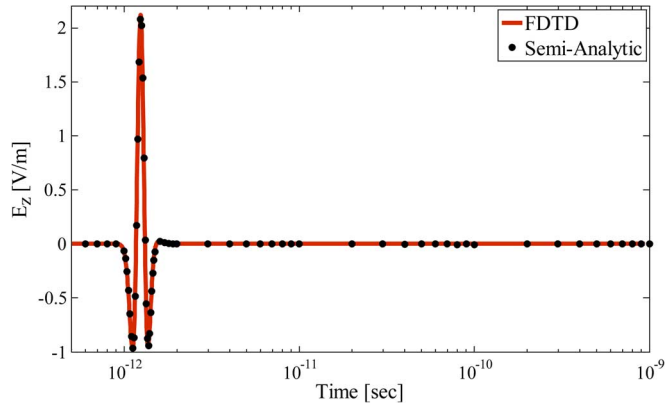

Fig. 5. E_z at the observation point, indicated by cross in Fig. 4, (c) normalized pattern of E_z at the wavelength of $\lambda_0 = 100$ μm.

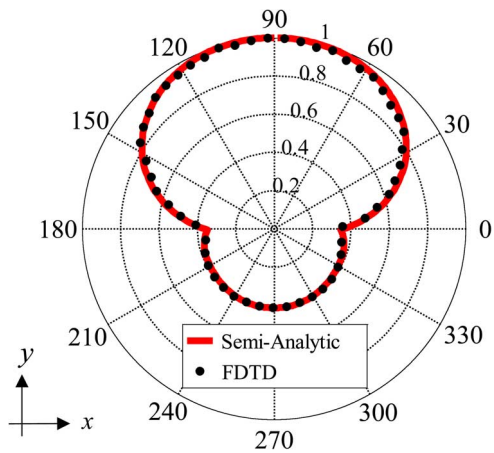

Fig. 6. Normalized pattern of E_z at the wavelength of $\lambda_0 = 100$ μm.

is used as the source. The electric field is recorded at both sides of the sheet and discrete Fourier transform (DFT) is used to obtain the transmission and reflection coefficients, which are also calculated analytically as $\mathrm{T} = 2/(2+\eta_0\sigma_g)$ and $\Gamma = \mathrm{T} - 1$, where η_0 is the free space impedance. The comparison between the results of our proposed FDTD algorithm and the analytic solution is shown in Fig. 3. By setting the FDTD spatial mesh to $\Delta z = \lambda_{\min}/20$ at 10 THz (and the time step to $\Delta t = \Delta z/\mathrm{c}_0$), the error between the FDTD and analytic solutions was found to be less than 0.035% in the amplitude and less than 0.8% in the phase, for all frequencies below 10 THz. Since the graphene was modeled as a boundary, the size of the FDTD mesh was chosen independently of the graphene sheet.

As a second example, we consider the 2-D problem of an infinite line source radiating next to an infinite graphene sheet, as shown in Fig. 4. The problem is simulated using 75×75 cells with $\Delta x = \Delta y = 2\mu$m with a 8-cells Berenger's original PML [17] to truncate the domain. To prevent reflection from PML, graphene boundary condition is extended into the PML such that H_x and its corresponding subcomponent of E_z are updated using the graphene boundary condition proposed here. To meet the CFL-stability condition, the time step is set to $\Delta t = \Delta x/(\sqrt{2}\mathrm{c}_0)$. A normal derivative Gaussian pulse having the waveform

$$I(t) = -\sqrt{(2\mathrm{e})}\beta(t - t_0)\exp\left\{-\beta^2(t - t_0)^2\right\}\ \mu\mathrm{A}$$

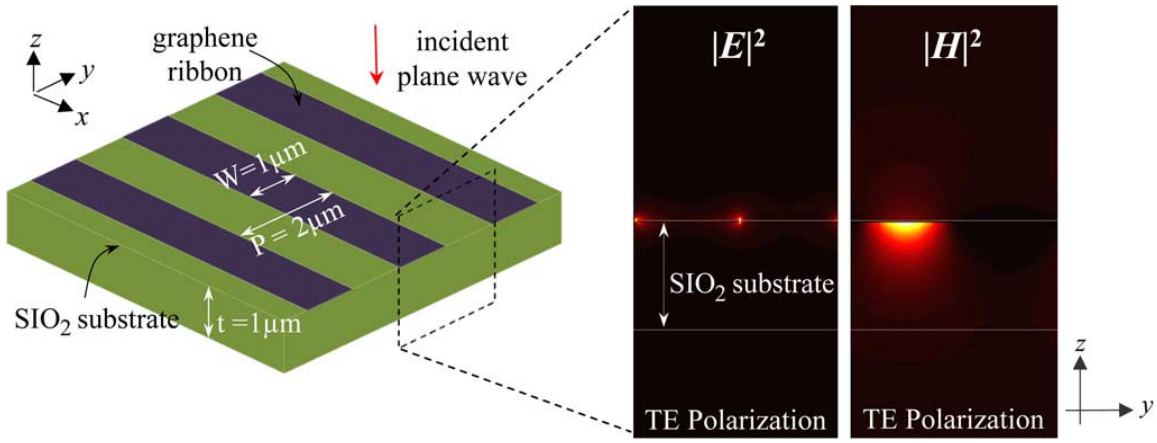

Fig. 7. Plane wave interaction with a periodic graphene micro-ribbon array supported by a SIO_2 thin film, inset showing intensity of the fields long after the pulse has passed the array for TE polarized excitation.

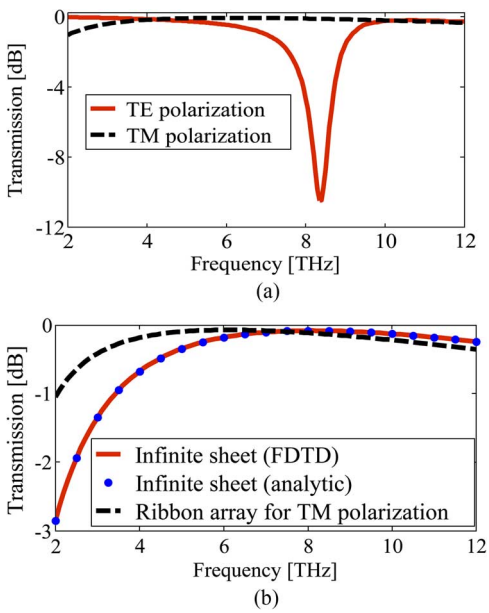

Fig. 8. (a) Transmission of the graphene micro-ribbon array for TE and TM polarized incident waves. (b) Comparison between transmission of the graphene micro-ribbon array for TM polarization with that of an infinite graphene sheet over the same substrate.

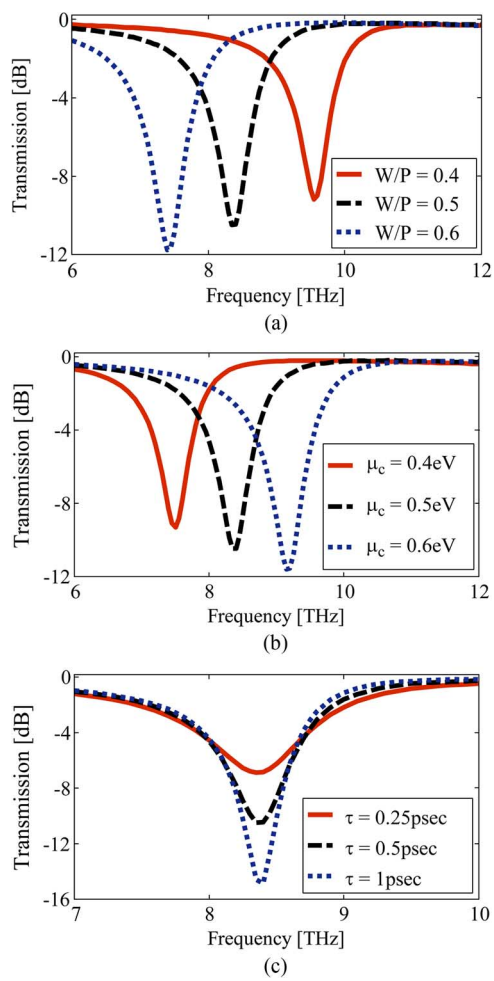

Fig. 9. Transmission of the graphene micro-ribbon array for TE polarized incident waves: (a) $\mu_c = 0.5$ eV, $\tau = 0.5$ ps and different values of W/P, (b) $\mathrm{W/P} = 0.5$, $\tau = 0.5$ ps and different values of μ_c, (c) $\mathrm{W/P} = 0.5$, $\mu_c = 0.5$ eV and different values of τ. In all results $\mathrm{P} = 2$ μm.

is used for the temporal excitation of the line source, where $t_0 = 1$ ps and $\beta = 10/t_0$. The values of E_z are recorded at observation circle depicted in Fig. 4. Fig. 5 shows the recorded E_z at the point depicted by cross in Fig. 4. Then DFT is used to obtain the pattern of E_z at the wavelength of $\lambda_0 = 100$ μm which is represented in Fig. 6. A semi-analytic solution is also obtained by approximating the grapheme sheet as a cylinder with a radius approaching infinity [31]. Fig. 5 and Fig. 6 show strong agreement between the FDTD results and those obtained from the semi-analytic method. Additionally, the applicability of classical PML to the proposed FDTD method is established in contrast to the subcell method where a special type of PML would be needed [21]. To test the stability of the method, the simulation was run for 200 000 time steps (around 1 ns) without any trace of instability.

Finally, we show the applicability of the proposed method to simulate finite-width graphene sheets. We consider periodic graphene micro-ribbon arrays recently reported in [32], [33]. Fig. 7 shows graphene ribbons, infinite in x and periodic in y. The computational domain consists of 101 Δy $\times$ 300 Δz cells with uniform cell size of 20 nm, and is terminated by periodic boundary condition and PML in the y and z directions,

respectively. A Gaussian waveform is used for the temporal excitation. The values of the transmitted fields are recorded and then DFT is used to obtain the frequency domain response. Fig. 8(a) shows the amplitude of the transmission coefficient for TE (magnetic field parallel to the ribbons) and TM (electric field parallel to the ribbons) polarized incident waves. For TM polarization, the transmission of the micro-ribbon array is similar to that of an infinite graphene sheet [which we calculated using our FDTD method and the analytic solution [34], and presented in Fig. 8(b)]; however for TE polarization, a stop band occurs around 8.35 THz due to plasmon resonance [32], [33] which is depicted in the inset in Fig. 7. Interestingly, in the stop band, the structure can be considered as a polarizer [35]. As shown in Fig. 9, the stop band frequency varies by changing W/L (see Fig. 7) and chemical potential (μ_c) and the bandwidth depends on the electron relaxation time (τ). We note here that in [33], the numerical solution was obtained using modal matching technique which is significantly limited in comparison to the FDTD method, especially when the number of graphene ribbons is finite or when using inhomogeneous substrates or coating.

V. Conclusion

This paper proposed a method for FDTD modeling of graphene. The graphene is considered as a zero-thickness conducting sheet and a novel approach based on coupling between updating equations at both sides of the sheet is used to implement a surface boundary condition in the FDTD method. Validation of the method is achieved by providing numerical examples and comparison with results obtained using analytic and semi-analytic solutions. Most importantly, the method proposed here for FDTD modeling of graphene is stable, reduces computational cost, and does not have sub-cell FDTD restrictions.

References

[1] A. K. Geim and K. S. Novoselov, "The rise of graphene," *Nature Mater.*, vol. 6, no. 3, pp. 183–191, Mar. 2007.

[2] K. S. Novoselov, V. I. Fal'ko, L. Colombo, P. R. Gellert, M. G. Schwab, and K. Kim, "A roadmap for graphene," *Nature*, vol. 490, no. 7419, pp. 192–200, Oct. 2012.

[3] G. W. Hanson, "Dyadic Green's functions and guided surface waves for a surface conductivity model of graphene," *J. Appl. Phys.*, vol. 103, no. 6, p. 064302, Mar. 2008.

[4] G. W. Hanson, "Dyadic Green's functions for an anisotropic, non-local model of biased graphene," *IEEE Trans. Antennas Propag.*, vol. 56, no. 3, pp. 747–757, Mar. 2008.

[5] A. Vakili and N. Engheta, "Transformation optics using graphene," *Science*, vol. 332, no. 6035, pp. 1291–1294, Jun. 2011.

[6] CST Studio Suite, [Online]. Available: http://www.cst.com

[7] COMSOL Multiphysics, [Online]. Available: http://www.comsol.com/

[8] W. Gao, J. Shu, C. Qiu, and Q. Xu, "Excitation of plasmonic waves in graphene by guided-mode resonances," *ACS Nano*, vol. 6, no. 9, pp. 7806–7813, Aug. 2012.

[9] Y. H. Kim, S. H. Kwon, J. M. Lee, M. S. Hwang, J. H. Kang, W. I. Park, and H. G. Park, "Graphene-contact electrically driven microdisk lasers," *Nature Commun.*, vol. 3, p. 1123, Oct. 2012.

[10] H. J. Xu, W. B. Lu, W. Zhu, Z. G. Dong, and T. J. Cui, "Efficient manipulation of surface plasmon polariton waves in graphene," *Appl. Phys. Lett.*, vol. 100, no. 24, p. 243110, Jun. 2012.

[11] A. Vakil and N. Engheta, "Fourier optics on graphene," *Phys. Rev. B*, vol. 85, no. 7, p. 075434, Feb. 2012.

[12] A. Andryieuski and A. V. Lavrinenko, "Graphene hyperlens for terahertz radiation," *Phys. Rev. B*, vol. 86, no. 12, p. 121108, Sep. 2012.

[13] N. Chamanara, D. Sounas, T. Szkopek, and C. Caloz, "Optically transparent and flexible graphene reciprocal and nonreciprocal microwave planar components," *IEEE Microw. Wireless Comp. Lett.*, vol. 22, no. 7, pp. 360–362, Jul. 2012.

[14] M. Tamagnone, J. S. Gomez-Diaz, J. R. Mosig, and J. Perruisseau-Carrier, "Analysis and design of terahertz antennas based on plasmonic resonant graphene sheets," *J. Appl. Phys.*, vol. 112, no. 11, p. 114915, Dec. 2012.

[15] I. Llatser, C. Kremers, A. Cabellos-Aparicio, J. M. Jornet, E. Alarcón, and D. N. Chigrin, "Graphene-based nano-patch antenna for terahertz radiation," *Photon. Nanost.—Fundament. Applic.*, vol. 10, no. 4, pp. 353–358, Oct. 2012.

[16] K. S. Yee, "Numerical solution of initial boundary value problems involving Maxwell's equations in isotropic media," *IEEE Trans. Antennas Propag.*, vol. AP-14, no. 3, pp. 302–307, May 1966.

[17] A. Taflove and S. Hagness, *Computational Electrodynamics: The Finite-Difference Time-Domain Method*. Norwood, MA, USA: Artech House, 1995.

[18] A. Mock, "Padé approximant spectral fit for FDTD simulation of graphene in the near infrared," *Opt. Mater. Exp.*, vol. 2, no. 6, pp. 771–781, Jun. 2012.

[19] H. Lim *et al.*, "FDTD modeling of graphene devices using complex conjugate dispersion material model," *IEEE Microw. Wireless Comp. Lett.*, vol. 22, no. 12, pp. 612–614, Dec. 2012.

[20] G. D. Bouzianas *et al.*, "Optimal modeling of infinite graphene sheets via a class of generalized FDTD schemes," *IEEE Trans. Magn.*, vol. 48, no. 2, pp. 379–382, Feb. 2012.

[21] X. Yu and C. D. Sarris, "A perfectly matched layer for subcell FDTD and applications to the modeling of graphene structures," *IEEE Antennas Wireless Propag. Lett.*, vol. 11, pp. 1080–1083, 2012.

[22] J. G. Maloney and G. S. Smith, "The use of surface impedance concepts in the finite-difference time-domain method," *IEEE Trans. Antennas Propag.*, vol. 40, no. 1, pp. 38–48, Jan. 1992.

[23] J. H. Beggs, R. J. Luebbers, K. S. Yee, and K. S. Kunz, "Finite-difference time-domain implementation of surface impedance boundary conditions," *IEEE Trans. Antennas Propag.*, vol. 40, no. 1, pp. 49–56, Jan. 1992.

[24] L. Wu and L. Han, "Implementation and application of resistive sheet boundary condition in the finite-difference time-domain method," *IEEE Trans. Antennas Propag.*, vol. 40, no. 6, pp. 628–633, Jun. 1992.

[25] J. G. Maloney and G. S. Smith, "A comparison of methods for modeling electrically thin dielectric and conducting sheets in the finite-difference time-domain method," *IEEE Trans. Antennas Propag.*, vol. 41, no. 5, pp. 690–694, May 1993.

[26] S. Van den Berghe, F. Olyslager, and D. De Zutter, "Accurate modeling of thin conducting layers in FDTD," *IEEE Microw. Wireless Comp. Lett*, vol. 8, no. 2, pp. 75–77, Feb. 1998.

[27] M. Sabrina Sarto, "A new model for the FDTD analysis of the shielding performances of thin composite structures," *IEEE Trans. Electromagn Compat.*, vol. 41, no. 4, pp. 298–306, Nov. 1999.

[28] W. Thiel, "A surface impedance approach for modeling transmission line losses in FDTD," *IEEE Microw. Wireless Compon. Lett.*, vol. 10, no. 3, pp. 89–91, Mar. 2000.

[29] M. Feliziani and F. Maradei, "Finite-difference time-domain modeling of thin shields," *IEEE Trans. Magn.*, vol. 36, no. 4, pp. 848–851, Jul. 2000.

[30] T. Stauber, N. M. R. Peres, and F. Guinea, "Electronic transport in graphene: A semiclassical approach including midgap states," *Phys. Rev. B*, vol. 76, no. 20, p. 205423, Nov. 2007.

[31] B. Alavikia and O. M. Ramahi, "Semianalytic solution to the problem of scattering from multiple cylinders above a perfectly conductive surface," *J. Opt. Soc. Amer. A*, vol. 28, no. 7, pp. 1489–1495, Jul. 2011.

[32] L. Ju *et al.*, "Graphene plasmonics for tunable terahertz metamaterials," *Nature Nanotechnol.*, vol. 6, no. 10, pp. 630–634, Sep. 2011.

[33] A. Y. Nikitin, F. Guinea, F. J. Garcia-Vidal, and L. Martin-Moreno, "Surface plasmon enhanced absorption and suppressed transmission in periodic arrays of graphene ribbons," *Phys. Rev. B*, vol. 85, no. 8, p. 081405, Feb. 2012.

[34] P. Y. Chen and A. Alù, "Atomically-thin surface cloak using graphene monolayers," *ACS Nano*, vol. 5, no. 7, pp. 5855–5863, Jun. 2011.

[35] H. Yan *et al.*, "Tunable infrared plasmonic devices using graphene/insulator stacks," *Nature. Nanotechnol.*, vol. 7, no. 5, pp. 330–334, Apr. 2012.

Vahid Nayyeri (S'08) was born in Tehran, Iran, in 1983. He received the B.Sc. degree from the Iran University of Science and Technology (IUST), Tehran, Iran, in 2006 and M.Sc. degree from the University of Teheran, Tehran, Iran, in 2008, both in electrical engineering. He is currently working toward the Ph.D. degree in electrical engineering at the Iran University of Science and Technology.

In September 2012, he joined the University of Waterloo as a Visiting Scholar. His research interests include computational electromagnetics, optimization methods, and bio electromagnetics.

Mr. Nayyeri has served as reviewer for the IEEE TRANSACTIONS ON ANTENNAS AND PROPAGATION and IEEE TRANSACTIONS ON MICROWAVE THEORY AND TECHNIQUES.

Mohammad Soleimani received the B.S. degree in electrical engineering from the University of Shiraz, Shiraz, Iran, in 1978 and the M.S. and Ph.D. degrees from Pierre and Marie Curio University, Paris, France, in 1981 and 1983, respectively.

Currently, he is a Professor with the Iran University of Sciences and Technology, Tehran, Iran. His research interests include computational electromagnetics and antennas.

Omar M. Ramahi (S'86–M'90–SM'00–F'09) was born in Jerusalem, Palestine. He received the B.S. degrees in mathematics and electrical and computer engineering (*summa cum laude*) from Oregon State University, Corvallis, OR, USA and the Ph.D. degree in electrical and computer engineering from the University of Illinois at Urbana-Champaign, Urbana, IL, USA, under the supervision of Prof. Raj Mittra.

He held post-doctoral and visiting fellowship positions at the University of Illinois at Urbana-Champaign under the supervision of Professors Y. T. Lo and Raj Mittra. He then worked at Digital Equipment Corporation (presently, HP), where he was a member of the Alpha Server Product Development Group. In 2000, he joined the faculty of the James Clark School of Engineering, University of Maryland at College Park, as an Assistant Professor and later as a tenured Associate Professor. At Maryland, he was also a faculty member of the CALCE Electronic Products and Systems Center. Currently, he is a Professor in the Electrical and Computer Engineering Department, University of Waterloo, ON, Canada. He holds cross appointments with the Department of Mechanical and Mechatronics Engineering and the Department of Physics and Astronomy. He has authored and coauthored over 300 journal and conference technical papers on topics related to the electromagnetic phenomena and computational techniques to understand the same. He is a coauthor of the book *EMI/EMC Computational Modeling Handbook,* (1st edition: Kluwer, 1998, 2nd ed: Springer-Verlag, 2001, Japanese edition published in 2005). He served as a consultant to several companies and was a cofounder of EMS-PLUS, LLC and Applied Electromagnetic Technology, LLC, and the Eastern Rugs and Gifts Company.

Prof. Ramahi is the winner of the 1994 Digital Equipment Corporation Cash Award, the 2004 University of Maryland Pi Tau Sigma Purple Cam Shaft Award for teaching, the Excellent Paper Award in the 2004 International Symposium on Electromagnetic Compatibility, Sendai, Japan, and the 2010 University of Waterloo Award for Excellence in Graduate Supervision. In 2012, he received the IEEE Electromagnetic Compatibility Society Technical Achievement Award. In 2009, he served as a Co-Guest Editor for the *Journal of Applied Physics* Special Issue on Metamaterials and Photonics. From 2009 to 2011, He served as IEEE EMC Society Distinguished Lecturer. Currently, he is serving as an Associate Editor for the IEEE TRANSACTIONS ON COMPONENTS, PACKAGING, AND MANUFACTURING TECHNOLOGY.